THE JOURNAL OF PHYSICAL CHEMISTRY C

ARTICLE

pubs.acs.org/JPCC

Potassium Zinc Borohydrides Containing Triangular $[Zn(BH_4)_3]^-$ and Tetrahedral $[Zn(BH_4)_xCl_{4-x}]^{2-}$ Anions

Radovan Černý,[*,†] Dorthe B. Ravnsbæk,[‡] Pascal Schouwink,[†] Yaroslav Filinchuk,[§] Nicolas Penin,[†,∥] Jeremie Teyssier,[⊥] L'ubomír Smrčok,[#] and Torben R. Jensen[‡]

[†]Laboratory of Crystallography, University of Geneva, 24, quai Ernest-Ansermet, CH-1211 Geneva, Switzerland

[‡]Center for Materials Crystallography (CMC), Interdisciplinary Nanoscience Center (iNANO), Department of Chemistry, Aarhus University, Langelandsgade 140, DK-8000 Århus C, Denmark

[§]Institute of Condensed Matter and Nanosciences, Université Catholique de Louvain, Place L. Pasteur, B-1348, Louvain-la-Neuve, Belgium

[∥]CNRS, Université de Bordeaux 1, ICMCB, 87, Avenue du Docteur Albert Schweitzer, F-33608 PESSAC Cedex, France

[⊥]Department of Solid State Physics, University of Geneva, 24, quai Ernest-Ansermet, CH-1211 Geneva, Switzerland

[#]Institute of Inorganic Chemistry, Slovak Academy of Sciences, Dúbravská cesta 9, SK-845 36 Bratislava, Slovak Republic

S *Supporting Information*

ABSTRACT: Three novel potassium−zinc borohydrides/chlorides are described. $KZn(BH_4)_3$ and $K_2Zn(BH_4)_xCl_{4-x}$ form in ball-milled KBH_4:$ZnCl_2$ mixtures with molar ratios ranging from 1.5:1 up to 3:1. On the other hand, $K_3Zn(BH_4)_xCl_{5-x}$ forms only in the 2:1 mixture after longer milling times. The new compounds have been studied by a combination of in situ synchrotron powder diffraction, thermal analysis, Raman spectroscopy, and the solid state DFT calculations. Rhombohedral $KZn(BH_4)_3$ contains an anionic complex $[Zn(BH_4)_3]^-$ with D_3 (32) symmetry, located inside a rhombohedron K_8. $KZn(BH_4)_3$ contains 8.1 wt % of hydrogen and decomposes at ∼385 K with a release of hydrogen and diborane similar to other Zn-based bimetallic borohydrides like $MZn_2(BH_4)_5$ (M = Li, Na) and $NaZn(BH_4)_3$. The decomposition temperature is much lower than for KBH_4. Monoclinic $K_2Zn(BH_4)_xCl_{4-x}$ contains a tetrahedral complex anion $[Zn(BH_4)_xCl_{4-x}]^{2-}$ located inside an Edshammar polyhedron (pentacapped trigonal prism) K_{11}. The compound is a monoclinically distorted variant of the paraelectric orthorhombic *ht*-phase of K_2ZnCl_4 (structure type K_2SO_4). $K_2Zn(BH_4)_xCl_{4-x}$ releases BH_4 starting from 395 K, forming Zn and KBH_4. As the reaction proceeds and *x* decreases, the monoclinic distortion of $K_2Zn(BH_4)_xCl_{4-x}$ diminishes and the structure transforms at 445 K into the orthorhombic *ht*-phase of K_2ZnCl_4. Tetragonal $K_3Zn(BH_4)_xCl_{5-x}$ is a substitutional and deformation variant of the tetragonal ($I4/mcm$) Cs_3CoCl_5 structure type possibly with the space group $P4_2/ncm$. $K_3Zn(BH_4)_xCl_{5-x}$ decomposes nearly at the same temperature as $KZn(BH_4)_3$, i.e., at ∼400 K, with the formation of $K_2Zn(BH_4)_xCl_{4-x}$ and KBH_4, indicating that the compound is an adduct of the two latter compounds.

INTRODUCTION

Bimetallic borohydrides currently attract significant attention due to their fascinating structural diversity and due to tunable physical properties.[1] A variety of new members of this group of compounds have been discovered during the past few years.[2] The preparation of bimetallic borohydrides was motivated by the idea of modifying the thermodynamic properties of stable alkali metal and alkali earth borohydrides by combining them with unstable transition metal borohydrides.[3] They are often prepared by mechanochemical methods (ball milling) from mixtures of alkali metal borohydrides and transition metal halides.[4]

Besides numerous reports on bimetallic borohydrides in the literature,[5−9] only three series of bimetallic borohydrides have been structurally characterized: $MSc(BH_4)_4$ (M = Li, Na, K),[10−12] $MZn_2(BH_4)_5$ (M = Li, Na) and $NaZn(BH_4)_3$,[13,14] and $Li_4Al_3(BH_4)_{13}$[15] as well as $NaAl(BH_4)_4$.[16] The aluminum compounds show partial solubility between the chloride and the borohydride anion. These compounds are described as salts containing complex anions such as tetrahedral $[Sc(BH_4)_4]^-$, $[Al(BH_4)_4]^-$, or triangular $[Zn(BH_4)_3]^-$. The $MZn_2(BH_4)_5$ (M = Li, Na) compounds may be rationalized as built of two interpenetrated frameworks containing a binuclear anion $[Zn_2(BH_4)_5]^-$. Ordered bimetallic borohydride-halides are also known, e.g., $KZn(BH_4)Cl_2$[17] and $NaY(BH_4)_2Cl_2$.[18]

In addition to bimetallic borohydrides with ordered structures, solid solutions of anion-substituted compounds may also be prepared,[19] and the first cationic solid solution borohydride $Mg_xMn_{1-x}(BH_4)_2$ was recently characterized.[20] In some systems there are no ternary compounds; for example, only eutectic melting mixtures were found in the systems $LiBH_4-Ca(BH_4)_2$[21] and $LiBH_4-Mg(BH_4)_2$.[22,23]

The present study tends to extend our knowledge about structural formation and evolution of bimetallic borohydrides within the $MM'-BH_4(Cl)$ series, where M is an alkali metal and M′ is a d-block metal. This has prompted the present investigation of potassium zinc borohydrides motivated in particular by the

Received: October 13, 2011
Revised: November 23, 2011
Published: November 29, 2011

Table 1. List of Prepared Samples, Phase Composition, and Agreement Factors (R_{wp} Corrected for Background) As Obtained by Rietveld Refinement (Program TOPAS) Using As-Milled Mixtures at Room Temperature[a]

sample	mixture KBH_4:$ZnCl_2$	$KZn(BH_4)_3$ [wt %]	$K_2Zn(BH_4)_xCl_{4-x}$ [wt%]	impurities [wt %]	R_{wp}	χ^2
A1	1.5:1	27.0(4)	73.0(4)	–	0.064	8450
A2	2:1	25.0(10)	33.0(30)	41.0(20) $K_3Zn(BH_4)_xCl_{5-x}$	0.240	127500
B2	2:1	18.5(6)	69.3(10)	8.6(4) KBH_4	0.090	9800
				3.6(9) β-$ZnCl_2$		
A3	2.667:1	15.6(6)	48.5(14)	27.4(8) KBH_4	0.078	2600
				8.5(8) β-$ZnCl_2$		
B4	3:1	14.1(5)	45.5(10)	31.0(8) KBH_4	0.092	6560
				9.4(9) β-$ZnCl_2$		

[a] Samples denoted **A** are prepared at the University of Geneva, and samples denoted **B** are prepared at Aarhus University. The high value of χ^2 reflects mainly the extremely high counting statistics of the powder diffraction data obtained from modern X-ray detectors

discovery of new compounds Li- and Na-containing analogues.[13] In the K-containing system, only a compound of composition $K_2Zn_3(BH_4)_8$ has been reported,[24,25] however without any structural details. We show that this compound does not form in ball-milled mixtures. Instead, three other salts are formed with the stoichiometries $KZn(BH_4)_3$, $K_2Zn(BH_4)_xCl_{4-x}$, and $K_3Zn(BH_4)_xCl_{5-x}$. Their powder patterns do not correspond to the patterns in Figure 3 of ref 25. We study the formation, structure, and decomposition pathways of the novel compounds and compare the results with recent studies of K−Mg−BH_4, K−Mn−BH_4,[26] and K−Cd−BH_4[27] systems.

EXPERIMENTAL SECTION

Sample Preparation. The preparation and manipulation of all samples were performed in an argon-filled glovebox with a circulation purifier ($p(O_2, H_2O) < 1$ ppm).

For samples **A** (prepared in Geneva, see Table 1), anhydrous zinc chloride, $ZnCl_2$ (Sigma-Aldrich, 99.995%), and potassium borohydride, KBH_4 (Sigma-Aldrich, 98%), were combined in molar ratios KBH_4:$ZnCl_2$ of 1.5:1, 2:1, and 2.667:1 and ball-milled under inert conditions (argon atmosphere) in a Fritsch Pulverisette 7 planetary mill for 350 min (5 min breaks every 10 min) using 25 mL stainless steel containers and an approximate 1:35 weight ratio of sample to three stainless steel balls with 15, 12, and 10 mm in diameter.

For samples **B** (prepared in Aarhus, see Table 1), anhydrous zinc chloride, $ZnCl_2$ (Sigma-Aldrich, ≥98%), and potassium borohydride, KBH_4 (Sigma-Aldrich, 98%), were combined in molar ratios KBH_4:$ZnCl_2$ of 2:1 and 3:1 and ball-milled for 120 min (2 min breaks every 2 min) under inert conditions (argon atmosphere) in a Fritsch Pulverisette 4 planetary mill using 80 mL tungsten carbide steel containers and an approximate 1:35 weight ratio of sample to 10 mm tungsten carbide steel balls.

Thermal Analysis. Simultaneous thermogravimetric analysis (TGA) and differential scanning calorimetry (DSC) were performed on samples **B** using a Netzsch STA449C Jupiter instrument and corundum crucibles with lids as sample holders. The samples were heated from RT to 500 °C (heating rate, $\Delta T/\Delta t$ = 10 °C/min). The experiments were conducted in a helium (4.6) atmosphere.

In Situ Time-Resolved Synchrotron Powder Diffraction (SR-PXD). In situ SR-PXD data for all samples were collected at the Swiss-Norwegian Beamlines (SNBL) at the European Synchrotron Radiation Facility (ESRF) in Grenoble, France. A glass capillary (o.d. 0.5 or 0.8 mm) with the sample was heated from RT to 400 or 500 K at a rate of 1 or 2 K/min while synchrotron powder diffraction data (SR-PXD) were collected. The temperature was controlled with the cooler Oxford Cryostream 700+. The data were collected on a MAR345 image plate detector using radiation with selected wavelengths of λ = 0.72846(2), 0.70351(2), or 0.69736(1) Å as determined by using external Si or LaB_6 standards. The capillary was oscillated by 1°/s during exposure to the X-ray beam for 20−60 s, followed by readout for ∼83 s. All obtained raw images were transformed to 2D-powder diffraction patterns using the FIT2D program.[28]

Structure Solution and Refinement. All measured powder patterns showed Bragg peaks of crystalline phases with fwhm within 0.1−0.2° 2θ.

$KZn(BH_4)_3$. The paraelectric high-temperature polymorph (s.g. *Pnma*) of K_2ZnCl_4 (structure type K_2SO_4)[29] was identified as a main phase in the SR-PXD data measured above 445 K for all samples. For the sample with the best crystallinity, sample **A3**, this allowed for subsequent identification of seven Bragg peaks belonging to an unknown phase, which disappear at ∼385 K. From the SR-PXD pattern measured at 100 K, these seven peaks were indexed with program FOX[30] in a hexagonal lattice with a = 7.6291(8), c = 10.977(2) Å, and V = 553.3(1) Å^3 (final values from Rietveld refinement at 100 K). The systematic extinctions pointed to a rhombohedral lattice. From the lattice parameters the structure type $KBrO_3$[31] was suggested with the composition $KZn(BH_4)_3$. The structure was solved with the direct space program FOX[30] and refined with the Rietveld method using the TOPAS program.[32] According to eqs 1 and 2, as given later, a borohydride-chloride, $K_2Zn(BH_4)_xCl_{4-x}$, unreacted KBH_4, and β-$ZnCl_2$ were introduced in the Rietveld refinement. The structures of KBH_4 and β-$ZnCl_2$ were based on the known structural models;[33] i.e., only the lattice parameters and isotropic displacement parameters were refined. The structural model of $K_2Zn(BH_4)_xCl_{4-x}$ as found from the powder diffraction data measured at higher temperatures (see below) was introduced in the refinement. The structure of $KZn(BH_4)_3$ was solved and refined with one BH_4 group as a semirigid ideal tetrahedron with refined B−H distance. The symmetry of the refined structure was subsequently checked with the routine ADDSYM of the program PLATON,[34] and the space group $R3$ was confirmed. This structural model of $KZn(BH_4)_3$ was optimized by DFT calculations in the solid state keeping the lattice parameters fixed to the values observed at 100 K. The DFT-optimized structure of $KZn(BH_4)_3$ fits very well powder diffraction data of all samples, and therefore only the atomic coordinates of the DFT-optimized structure at 100 K are given in Supporting Information Table S1

and as a CIF file. The lattice parameters at RT are also given in Table S1 (Supporting Information) as refined from the powder diffraction data of the sample **A1**.

$K_2Zn(BH_4)_xCl_{4-x}$. The diffraction peaks observed in the powder pattern of the sample **B1** at 500 K were identified as belonging to the orthorhombic (*Pnma*) *ht*-K_2ZnCl_4. These peaks split with decreasing temperature indicating a monoclinic distortion with lattice parameters a = 12.363(4), b = 9.110(3), c = 7.339(2) Å, β = 95.74(2)°, and V = 822.5(4) Å^3 (final values from Rietveld refinement at 100 K). The space group was determined from the systematic extinctions as $P2_1/n$ (nonstandard setting of the space group $P2_1/c$) indicating that the compound is a monoclinic deformation of *ht*-K_2ZnCl_4. The structural model of $K_2Zn(BH_4)_xCl_{4-x}$ was obtained from the SR-PXD data of sample **A3** measured at 400 K by searching direct space in FOX, starting out from the orthorhombic prototype *ht*-K_2ZnCl_4 (space group setting *Pbnm*) transformed to monoclinic symmetry of $P2_1/n$ and mixing the Cl atoms with BH_4 groups. The final refinement was carried out using the SR-PXD pattern for sample **A3** measured at 100 K. This sample was preferred over the sample **A1**, even though the weight fraction of $K_2Zn(BH_4)_xCl_{4-x}$ is higher in the latter (see Table 1). Higher content of borohydride, x = 1.9, in sample **A3** compared to x = 0.92 in sample **A1** and stronger monoclinic deformation made the sample **A3** more suitable for the final refinement. Four antibump distance restraints were needed to stabilize the refinement of $K_2Zn(BH_4)_xCl_{4-x}$, i.e., Zn−H 1.9, Zn−B 2.5, K−B 3.2, and H−H 2.2 Å. Three isotropic displacement parameters (two for K and Zn and one for B, H, and Cl) were refined. The structure of $KZn(BH_4)_3$ was fixed to the DFT-optimized model, and only three isotropic displacement parameters (two for K and Zn and one for B and H) were refined. The uncertainties of crystallographic coordinates of borohydrides were not available from the least-squares matrix and were estimated by the bootstrap method.[35] The agreement factors from the Rietveld refinement using the sample **A3** at 100 K are the following: R_{wp} (not corrected for background) = 4.56%, R_{wp} (corrected for background) = 8.84%, $\chi^2 = 1.8 \times 10^4$, R_{Bragg} ($KZn(BH_4)_3$) = 1.58%, and R_{Bragg} ($K_2Zn(BH_4)_xCl_{4-x}$) = 1.76%. The high value of χ^2 reflects mainly the extremely high counting statistics of the powder diffraction data obtained from modern 2D detectors. The refined structural parameters of $K_2Zn(BH_4)_xCl_{4-x}$ at 100 K are given in Table S2 (Supporting Information) and as a CIF file, and the Rietveld plot is shown in Figure S1 (Supporting Information). The lattice parameters at RT for borohydride contents of x = 1.9 and x = 0.92 are also given in Table S2 (Supporting Information) as refined from the powder diffraction data of the sample **A3** and **A1**, respectively.

DFT Calculation. The solid state DFT calculations were performed using the VASP program.[36,37] The electron exchange-correlation interaction was described in the generalized gradient approximation PW91 according to Perdew and Wang.[38] Plane waves formed the basis set, and calculations were performed using the projector-augmented wave method[39,40] and atomic pseudopotentials.[41] The energy cutoff controlling the accuracy of the calculation was set to 500 eV, representing an extended basis set and consequently highly accurate calculations. The positions of all atoms were optimized by means of the conjugated gradient method in the four k-points[42,43] with the unit cell parameters fixed. Considering the size of the unit cell, the calculations were restricted to the gamma point of the Brillouin zone. The normal modes were calculated in the harmonic approximation with the total energy converged to 10^{-7} eV and with the residual forces on the atoms smaller than 0.005 eV/Å. The Hessian was constructed from the single-point energy calculations of the 6n structures generated from the optimized structure by displacing each of the n atoms in the cell in the positive and negative senses along the Cartesian directions x, y, and z.[44] The calculated modes were analyzed with the help of the MOLEKEL program.[45]

Raman Spectroscopy. Raman spectra were collected on the sample **A1** using a homemade micro Raman spectrometer equipped with an argon laser at a wavelength of 514.5 nm, a 50 × long distance working objective, a nitrogen-cooled CCD detector, and helium cryostat. The low signal to background ratio is due to the extremely low power used for these experiments (600 μW) as the sample showed high sensitivity to the laser beam. To protect samples from the air, powders were loaded into XRD sample holders and covered with a transparent foil. To remove the Raman signal of the foil, we opted for a 63 × long working distance objective, focusing through the foil onto a half-filled sample holder. Each presented spectrum is an average of 1000 spectra of 1 s exposure.

RESULTS AND DISCUSSION

Synthesis and Initial Phase Analysis. Ball milling of all KBH_4:$ZnCl_2$ mixtures results in the formation of a new bimetallic borohydride $KZn(BH_4)_3$ described by the reaction scheme 1

$$3KBH_4 + ZnCl_2 \rightarrow KZn(BH_4)_3 + 2KCl \quad (1)$$

A consecutive reaction 2 produces a ternary chloride K_2ZnCl_4

$$2KCl + ZnCl_2 \rightarrow K_2ZnCl_4 \quad (2)$$

as concluded from the formation of this compound in all mixtures.

However, K_2ZnCl_4 formed by the reaction 2 contains BH_4 substituting for Cl (see below). The ideal ratio for the maximum yield of $KZn(BH_4)_3$ lies therefore between KBH_4:$ZnCl_2$ = 1.5:1 and 2:1, depending on the solubility x of BH_4 in $K_2Zn(BH_4)_xCl_{4-x}$. Sample **A1** (KBH_4:$ZnCl_2$ = 1.5:1) yielded 27 wt % $KZn(BH_4)_3$ and 73 wt % $K_2Zn(BH_4)_xCl_{4-x}$ (see Table 1). There is an excess of KBH_4 in other samples, hence unreacted KBH_4 is observed. Traces of metallic zinc and one unidentified weak diffraction peak ($d \sim 3.42$ Å) were observed in the as-milled samples **A1** and **A3** indicating that additional intermediate compounds may form during the reactions 1 and 2.

Interestingly, sample **A2** shows diffraction peaks from one additional compound compared to the sample **B2** (both mixtures in the ratio KBH_4:$ZnCl_2$ = 2:1, see Figure S2 in Supporting Information). This compound is derived from the tetragonal ($I4/mcm$) structure type Cs_3CoCl_5[46] and has the composition $K_3Zn(BH_4)_xCl_{5-x}$ (see below). The conditions for the formation of $K_3Zn(BH_4)_xCl_{5-x}$ may be realized only in a very narrow composition range as it was observed only in the sample **A2**. The absence of this compound in the sample **B2** may arise from different ball milling conditions. The main difference between these two samples mixed with the same ratio KBH_4:$ZnCl_2$ = 2:1 (see Table 1) is the total ball milling time, i.e., 120 and 350 min for samples **B** and **A**, respectively. We conclude that with longer ball milling time the $K_2Zn(BH_4)_xCl_{4-x}$ produced by reaction

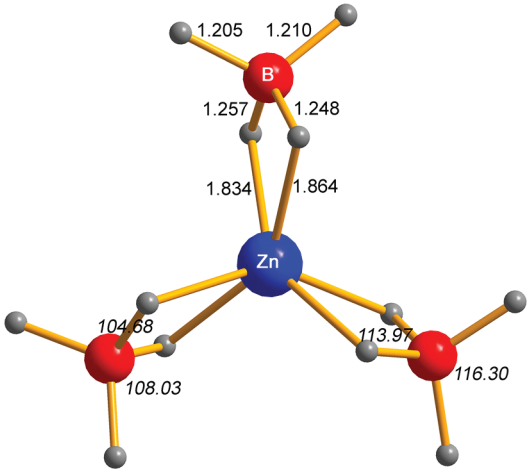

Figure 1. Triangular anionic complex $[Zn(BH_4)_3]^-$ with the symmetry D_3 (32) in the crystal structure of $KZn(BH_4)_3$ (space group $R3$) as observed by Rietveld refinement and DFT calculations. Interatomic distances (Å) are shown in regular font, bond angles (°) in italics. All structural drawings were prepared with the program DIAMOND.[57]

2 starts to react with the remaining KBH_4 according to

$$K_2Zn(BH_4)_xCl_{4-x} + KBH_4 \rightarrow K_3Zn(BH_4)_{x+1}Cl_{4-x} \quad (3)$$

Crystal Structure of $KZn(BH_4)_3$. The crystal structure of the new bimetallic borohydride $KZn(BH_4)_3$, which forms in all mixtures, can be derived from the structure type $KBrO_3$ with Zn placed on the Br position and BH_4 on the O position. Zn is coordinated by three BH_4 groups in a triangular planar coordination (deviation of the Zn atom from the plane of three B atoms is 0.09 Å), suggesting the anionic complex $[Zn(BH_4)_3]^-$ (Figure 1). The complex is located inside a rhombohedron K_8 with the rhombohedral angle of 83.54° (Figure 2) and has the symmetry of D_3 (32) with Zn−B distances of 2.199 Å and bidentate bonding mode $Zn-H_2BH_2$. However, the space group symmetry of $KZn(BH_4)_3$ is not $R32$ but $R3$ because the 2-fold axis of the complex anion is not collinear with the 2-fold axes in $R32$, and the complex is located on the Wyckoff site 3*a* with point symmetry 3. The Zn-coordinated H−H edges of three BH_4 tetrahedra are not perpendicular to the plane of three B atoms but are rotated by 16.1° (see Figure 1) to minimize repulsive H−H interactions (H−H > 2.65 Å). Similarly, a conrotation angle of 23° is observed for the molecular $Al(BH_4)_3$ by infrared spectroscopy and ab initio calculations.[47] The inner (Zn-coordinated H) B−H distances are longer (1.248 and 1.257 Å) than the outer B−H distances (1.205 and 1.210 Å). The latter compare well with the typical B−H distances in metal borohydrides as resulting from DFT calculations[48] or observed by neutron diffraction.[49] The H−B−H angle is 113.97° and 116.30° for $Zn-H_2B$ and $K-H_2B$ fragments, respectively, while it is within 104.68−108.03° for the noncoordinating H_2B edges. A similar opening of the coordinating H_2B edges of the complex anion $[Zn(BH_4)_3]^-$ was observed by DFT calculations in $NaZn(BH_4)_3$[14] as well as of the complex anion $[Zn_2(BH_4)_5]^-$ in $LiZn_2(BH_4)_5$[49] by neutron powder diffraction, and it is known for several binary borohydrides (see Discussion in ref 49).

The complex anion $[Zn(BH_4)_3]^-$ in $KZn(BH_4)_3$ has triangular geometry very similar to the one found in monoclinic $NaZn(BH_4)_3$[14] (see Figure 2). An important difference in the case of

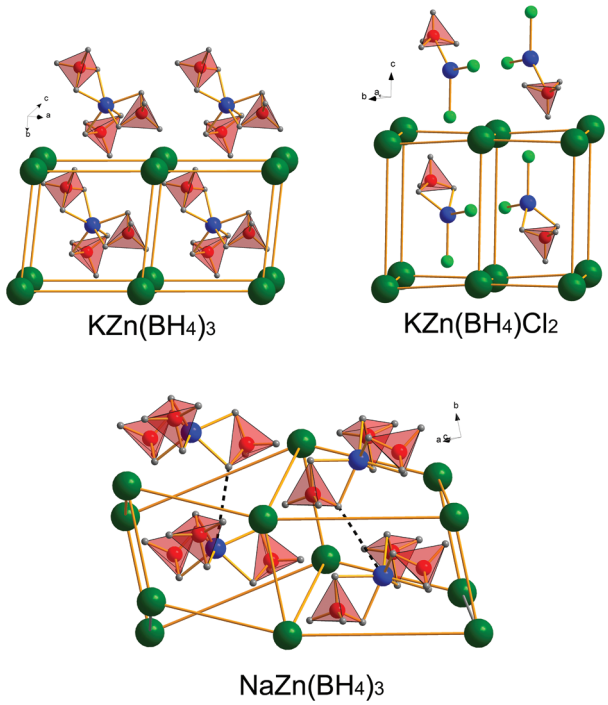

Figure 2. Fragments of crystal structures of $KZn(BH_4)_3$ (space group $R3$), $KZn(BH_4)Cl_2$ (space group $P2_1/m$), and $NaZn(BH_4)_3$ (space group $P2_1/c$) showing triangular complex anions $[Zn(BH_4)_3]^-$ and $[Zn(BH_4)Cl_2]^-$ located in alkali metal cage M_8. Black dashed lines show a lengthened axial contact associating the anions into a chain.

$NaZn(BH_4)_3$ is the orientation of one BH_4 tetrahedron: the Zn-coordinated H−H edge is exactly perpendicular to the plane of the three B atoms with two other tetrahedra staying inclined and thus breaking the D_3 (32) symmetry of the complex hydride anion. The BH_4 tetrahedron perpendicular to the plane has the shortest contact distance to neighboring complex anion $[Zn(BH_4)_3]^-$ (black dashed line in Figure 2) which originally motivated the rationalization of $NaZn(BH_4)_3$ as built from 1D polymeric anions $[\{Zn(BH_4)_3\}_n]^{n-}$[13]. Indeed, it is this interaction which may have the origin in the smaller Na^+ cation compared to the K^+ cation and consequently resulting in the lower symmetry of the complex anion $[Zn(BH_4)_3]^-$ and of the whole crystal structure of $NaZn(BH_4)_3$ compared to $KZn(BH_4)_3$. The coordinating rhombohedron K_8 of $KZn(BH_4)_3$ becomes a strongly deformed tetragonal prism Na_8 in $NaZn(BH_4)_3$ (Figure 2). A triangular heteroleptic complex anion $[Zn(BH_4)Cl_2]^-$ has been observed in $KZn(BH_4)Cl_2$,[17] which forms in the ball-milled mixtures KBH_4:$ZnCl_2$ with molar ratio of 1:1. The complex is positioned on a mirror plane, i.e., it is planar, and is located inside slightly deformed tetragonal prism K_8 (Figure 2).

A ternary borohydride with the stoichiometry 1:1:3 has been recently observed also in the $K-Mn-BH_4$[26] and $K-Cd-BH_4$ systems,[27] however, with different crystal structures of framework types. Cadmium is situated in $KCd(BH_4)_3$ in two different coordinations to BH_4 with higher coordination numbers, tetrahedral and octahedral, compared to zinc in $KZn(BH_4)_3$. Manganese is situated in perovskite-derived $KMn(BH_4)_3$ in octahedral coordination.

Replacing the anions $[Zn(BH_4)_3]^-$ in $KZn(BH_4)_3$ by a monatomic anion B the structure type *rt*-GeTe is obtained,[50] which is a distortion variant of the rhombohedral *rt*-NiO structure type, which is itself a distortion of the close-packed NaCl-type.

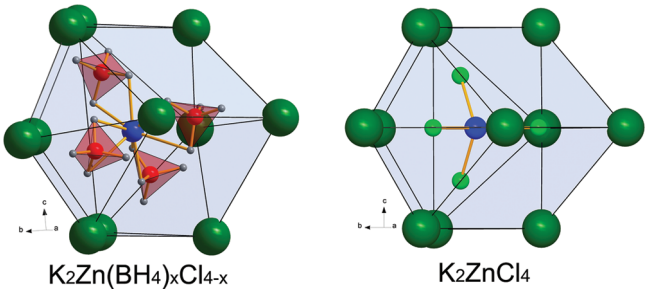

Figure 3. Tetrahedral anionic complexes in an Edshammar polyhedron (pentacapped trigonal prism) K_{11}: (left) $[Zn(BH_4)Cl_4]^{2-}$ in $K_2Zn(BH_4)_xCl_{4-x}$ (s.g. $P2_1/n$); (right) $[ZnCl_4]^{2-}$ in *ht*-phase of K_2ZnCl_4 (structure type K_2SO_4, s.g. setting *Pbnm*).

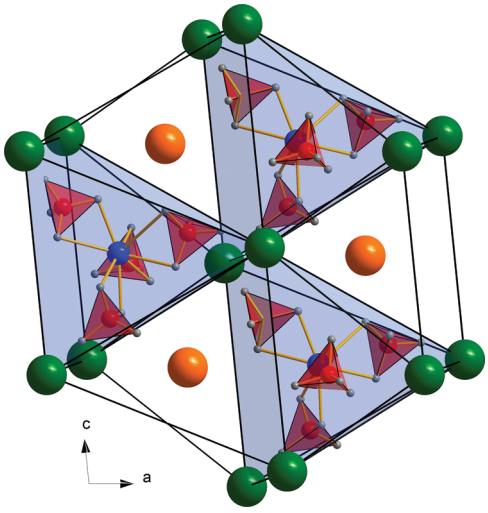

Figure 4. Crystal structure of $K_2Zn(BH_4)_xCl_{4-x}$ viewed along the *b*-axis, showing the relation to the Ni_2In and NiAs structure types: green K atoms (K2) make slightly deformed trigonal prisms. As in $NaSc(BH_4)_4$,[11] each second prism contains the complex anion - similarity to NiAs type. In $K_2Zn(BH_4)_xCl_{4-x}$, the rest of the prisms are filled by the second K atom (K1, orange) - similarity to Ni_2In type.

Crystal Structure of $K_2Zn(BH_4)_xCl_{4-x}$. The structure of $K_2Zn(BH_4)_xCl_{4-x}$ is a monoclinically distorted variant of the *ht*-phase of K_2ZnCl_4 (structure type K_2SO_4) which is stable above 555 K.[29] Figure 3 compares the coordination of the complex anion $[Zn(BH_4)_xCl_{4-x}]^{2-}$ and $[ZnCl_4]^{2-}$ in $K_2Zn(BH_4)_xCl_{4-x}$ and K_2ZnCl_4, respectively. The coordination polyhedron is a deformed Edshammar polyhedron,[51] i.e., pentacapped trigonal prism K_{11}. The polyhedron is deformed mostly in the equatorial plane of the prism. The lattice expansion at RT induced by the borohydride substitution is strongly anisotropic with maximal expansion along the *c*-axis and the monoclinic angle rapidly increasing to ~94° already for $x = 0.92$.

A ternary borohydride with a stoichiometry 2:1:4 has been recently observed also in K−Mg−BH_4, K−Mn−BH_4,[26] and K−Cd−BH_4 systems.[27] All of these compounds contain a complex anion $[M'(BH_4)_4]^{2-}$ (M′ = Mg, Mn, or Cd) located in the deformed Edshammar polyhedron K_{11}. The compounds differ in the degree of deformation of the pentacapped trigonal prism and consequently in the coordination numbers of two K sites. More detailed analysis is given in ref 26.

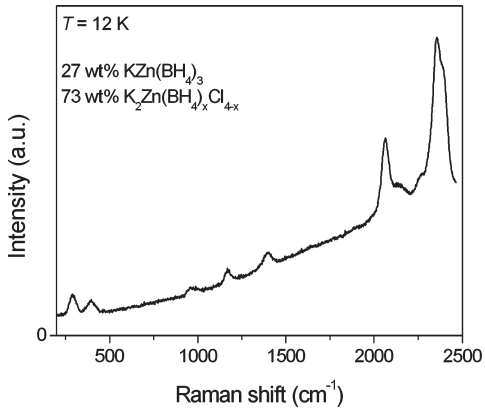

Figure 5. Raman spectrum of the sample **A1** measured at $T = 12$ K. The sample contains 27 wt % $KZn(BH_4)_3$ and 73 wt % $K_2Zn(BH_4)_xCl_{4-x}$ as obtained from Rietveld refinement.

If the complex anion $[Zn(BH_4)_xCl_{4-x}]^{2-}$ is replaced by a monatomic anion B, a binary compound K_2B is obtained whose high symmetry prototype is hexagonal Ni_2In structure type (s.g. $P6_3/mmc$)[52] derived from the NiAs structure type by filling trigonal prismatic interstices As_6 by Ni. A projection of $K_2Zn(BH_4)_xCl_{4-x}$ along the *b*-axis showing this packing is given in Figure 4. Interestingly, NiAs structure type represents a high-symmetry prototype of the Na^+ and $[Sc(BH_4)_4]^-$ packing in $NaSc(BH_4)_4$ (see Figure 13 in ref 11). A series of structures related to the Ni_2In *aristo*-type by group−subgroup relation is known for binary ionic compounds A_2B.[53] A structural drawing of $K_2Zn(BH_4)_xCl_{4-x}$ directly comparable with $K_2Cd(BH_4)_4$ (Figure 2c in ref 27) is given in the Supporting Information as Figure S3.

While $KZn(BH_4)_3$ is clearly rationalized as a salt containing a complex anion $[Zn(BH_4)_3]^-$, the understanding of bonding in $K_2Zn(BH_4)_xCl_{4-x}$ is not that straightforward. The ternary chloride K_2ZnCl_4 has been described as containing a complex anion $[ZnCl_4]^{2-}$.[29] The distances Zn−B/Cl become longer and K−B/Cl shorter in $K_2Zn(BH_4)_xCl_{4-x}$ compared to K_2ZnCl_4 (Table S3, Supporting Information), the latter being shorter than the K−B distances in $KZn(BH_4)_3$ and KBH_4. A description of $K_2Zn(BH_4)_xCl_{4-x}$ as a 3D polymeric structure should not be therefore excluded.

K_2ZnCl_4 was reported[29] to transform to a ferroelectric orthorhombic ($Pna2_1$) phase below 555 K with three times larger cell volume, which is incommensurately modulated between 403 and 555 K. Interestingly, the BH_4 substitution for Cl suppresses the 3-fold structure within the studied temperature range (up to 500 K).

Crystal Structure of $K_3Zn(BH_4)_xCl_{5-x}$. Comparing the lattice parameters, it was found that the structure of $K_3Zn(BH_4)_xCl_{5-x}$ may be derived from the tetragonal ($I4/mcm$) structure type Cs_3CoCl_5.[46] A compound with this structure type exists in a Zn-containing system as Cs_3ZnBr_5.[54] The composition of this additional compound is therefore estimated as K_3ZnCl_5; however, the symmetry is lower than $I4/mcm$, likely a consequence of BH_4 substitution on Cl sites. The most probable space group is $P4_2/ncm$ (maximal subgroup of $I4/mcm$) as suggested from the analysis of systematic extinctions. A compound with the same stoichiometry was recently identified in the K−Mg−BH_4 system,[26] however, with different deformation of the Cs_3CoCl_5 structure type having space group $P4_2/mbc$. The structure of $K_3Zn(BH_4)_xCl_{5-x}$ is not yet fully characterized; see Supporting Information

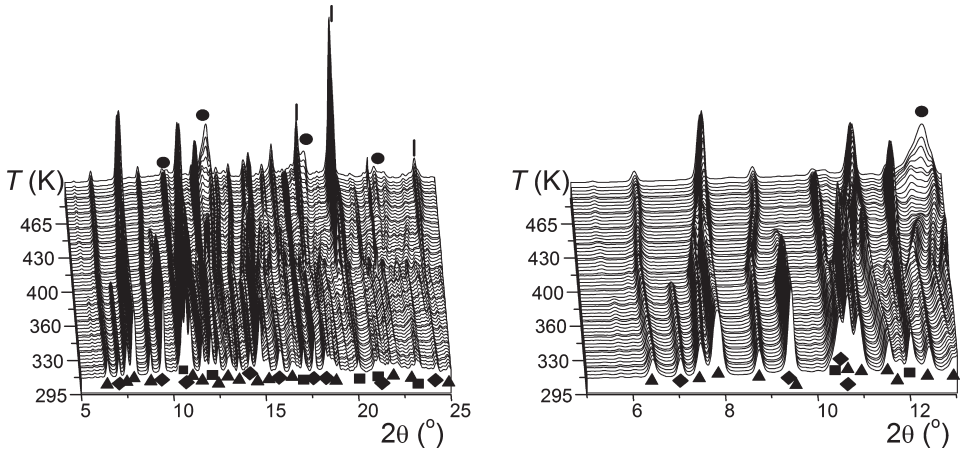

Figure 6. In situ SR-PXD data (left) measured for a ball-milled sample of KBH_4-ZnCl_2 in molar ratio 2:1 (sample **B2**) from RT to 500 K, $\Delta T/\Delta t = 1$ K/min (ESRF, $\lambda = 0.70351(2)$ Å). The right plot shows an enlargement of the in situ SR-PXD data. Symbols: ◆ $KZn(BH_4)_3$, ■ $K(BH_4)_xCl_{1-x}$, ▲ $K_2Zn(BH_4)_xCl_{4-x}$, ● KCl and Zn.

(Figures S4 and S5) for more details. From the analogy with the $K-Mg-BH_4$ system we may, however, conclude that the compound contains a complex anion $[Zn(BH_4)_xCl_{4-x}]^{2-}$.

Raman Spectroscopy. A Raman spectrum measured at 12 K on the sample **A1** is shown in Figure 5. The interpretation of the spectrum is complicated by the presence of two borohydride/chloride compounds in the sample, i.e., 27 wt % $KZn(BH_4)_3$ and 73 wt % $K_2Zn(BH_4)_xCl_{4-x}$. The spectrum nevertheless resembles the experimental spectrum (measured at 77 K) of $KZn(BH_4)Cl_2$[17] containing the triangular anion $[Zn(BH_4)Cl_2]^-$ and experimental RT spectrum of $NaZn(BH_4)_3$[14] containing the triangular anion $[Zn(BH_4)_3]^-$. On the other hand, the stretching modes in the spectrum resemble also the experimental RT spectrum of the sample containing $K_2Mn(BH_4)_4$ as the main phase.[26] We may therefore explain the measured Raman spectrum in the stretching mode as a superposition of two split stretching modes arising from two complex anions: $[Zn(BH_4)_3]^-$ and $[Zn(BH_4)_xCl_{4-x}]^{2-}$. The weak band at ~400 cm^{-1} is another signal of a complex anion in the sample.[14] Three bands between ~960 and 1410 cm^{-1} were assigned to bidentate bridging $B-H-Zn$ bending mode in $NaZn(BH_4)_3$.[14] The sharp band at ~290 cm^{-1} can be assigned to the stretching $Zn-Cl$ mode in $K_2Zn(BH_4)_xCl_{4-x}$.[55]

Decomposition Analysis by in Situ SR-PXD. In situ SR-PXD data on the sample **B2** indicate a decomposition of $KZn(BH_4)_3$ at ~385 K (see Figure 6). At the same temperature, the amount of $K_2Zn(BH_4)_xCl_{4-x}$ in the sample increases, and formation of metallic Zn is observed. The BH_4 content in $K_2Zn(BH_4)_xCl_{4-x}$ extracted from a Rietveld refinement increases and along with the release of B_2H_6 suggested by the TGA measurement (see below) allows us to formulate the idealized decomposition reaction as

$$2KZn(BH_4)_3 \rightarrow K_2Zn(BH_4)_4 + Zn + B_2H_6 + H_2 \quad (4)$$

Release of B_2H_6 and H_2 gas and a formation of metallic Zn have previously been observed for a ball-milled $2NaBH_4-ZnCl_2$ sample.[56] At higher temperatures, from 395 to 465 K, the BH_4 content in $K_2Zn(BH_4)_xCl_{4-x}$ is decreasing simultaneously with a formation of Zn and KBH_4 possibly due to the following idealized reaction

$$4K_2Zn(BH_4)_xCl_{4-x} \rightarrow (4-x)K_2ZnCl_4 + xKBH_4 + xZn \quad (5)$$

As the reaction 5 proceeds and x decreases, the monoclinic distortion of $K_2Zn(BH_4)_xCl_{4-x}$ decreases, and the structure transforms at 445 K into the symmetry of the orthorhombic *ht*-phase K_2ZnCl_4, which is stabilized below 555 K by the residual BH_4 substitution. This is confirmed by comparing the $K_2Zn(BH_4)_xCl_{4-x}$ cell volume of 825 $Å^3$ at 445 K with that of 820 $Å^3$ reported for K_2ZnCl_4 at 453 K.[29] The temperature evolutions of the monoclinic lattice parameter β and of the cell volume V of $K_2Zn(BH_4)_xCl_{4-x}$ are shown in Figure 7.

Upon further heating KBH_4 reacts with K_2ZnCl_4 to release B_2H_6 and H_2 and yield Zn and KCl according to the reaction

$$K_2ZnCl_4 + 2KBH_4 \rightarrow Zn + B_2H_6 + H_2 + 4KCl \quad (6)$$

Similar reactions have been observed during decomposition of $MZn_2(BH_4)_5$ (M = Li, Na) and $NaZn(BH_4)_3$.[13,14] KCl formed in reaction 6 is simultaneously substituted into the remaining KBH_4 yielding $K(BH_4)_xCl_{1-x}$ much like in the MBH_4-ScCl_3 (M = Na or K) systems.[11,12]

In situ SR-PXD data of sample **A1** (ratio KBH_4:$ZnCl_2$ of 1.5:1) reveal that the monoclinic distortion in $K_2Zn(BH_4)_xCl_{4-x}$ is strongly decreasing with increasing temperature already before the decomposition of $KZn(BH_4)_3$ (see Supporting Information, Figure S6). This is because of low BH_4 content of $x = 0.92$ in $K_2Zn(BH_4)_xCl_{4-x}$ in the as-milled mixture compared to the sample **B2** with $x = 1.26$. When $KZn(BH_4)_3$ decomposes, the monoclinic distortion and the cell volume in $K_2Zn(BH_4)_xCl_{4-x}$ increase again due to the dissolution of BH_4 and then decrease with further heating (see Figure S6, Supporting Information) because of BH_4 release, similarly to the sample **B2** (see Figure 6).

As observed from the in situ SR-PXD data of sample **A2**, $K_3Zn(BH_4)_xCl_{5-x}$ decomposes nearly at the same temperature as $KZn(BH_4)_3$, i.e., at ~400 K (Figure S7, Supporting Information), simultaneously with an increase in the diffracted intensity of $K_2Zn(BH_4)_xCl_{4-x}$ and KBH_4 in agreement with the reversed direction of reaction 3.

Thermal Analysis. Figure 8 shows the TGA and DSC data for the ball-milled samples of **B2** and **B4** (KBH_4:$ZnCl_2$ = 2:1 and 3:1, respectively). These data demonstrate that the decomposition has a multistep pathway. For both samples, a mass loss is observed in the TGA data at 400 K accompanied by a sharp DSC peak followed by a very broad endothermic peak in the DSC

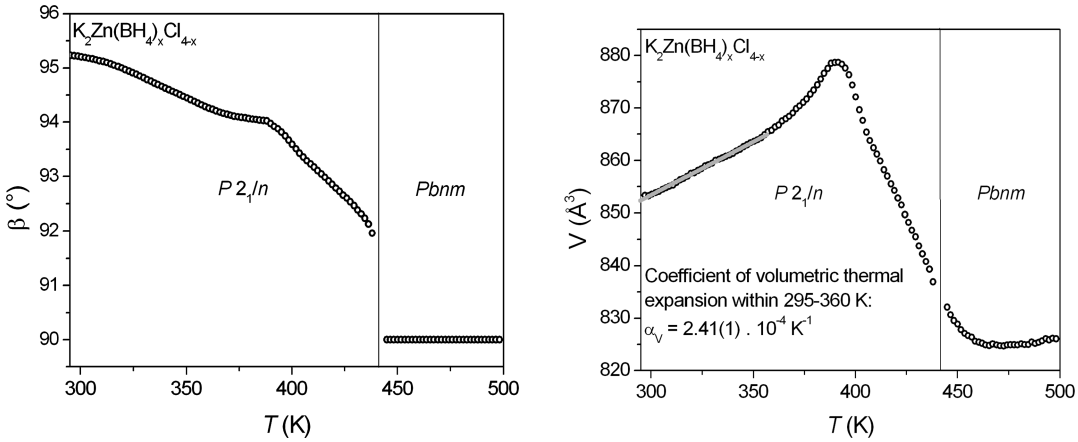

Figure 7. Thermal evolution of the monoclinic angle β and of the cell volume V of $K_2Zn(BH_4)_xCl_{4-x}$ illustrating the evolution from the monoclinic ($P2_1/n$) to the orthorhombic ($Pbnm$) phase. A volumetric thermal expansion coefficient is determined from the linear fit (shown in light gray) of V vs T between 295 and 360 K. The data are taken from the Rietveld refinement on the sample **B2**. Cell volume increase between 385 and 395 K is related to the increase of BH_4 content according to reaction 4, and the cell volume decrease above 395 K is related to the decrease of BH_4 content according to reaction 5.

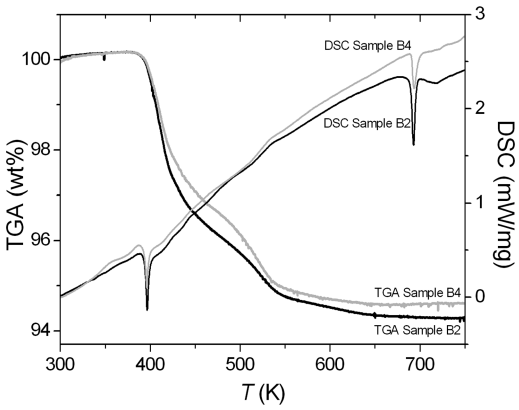

Figure 8. Thermal analysis (TGA and DSC) of samples **B2** (black curves) and **B4** (gray curves), corresponding to KBH_4-ZnCl_2 mixtures in molar ratios 2:1 and 3:1, respectively.

signal. The mass losses observed are 3.68 and 3.20 wt % for sample **B2** and **B4**, respectively. Since the DSC peak and the mass loss occur at the same temperature as the decomposition observed by in situ SR-XPD, we conclude that these effects take an origin in the decomposition of $KZn(BH_4)_3$. The lower mass loss for the sample **B4** is due to the presence of the residual KBH_4 in the sample.

Upon further heating, a second mass loss and a broad endothermic peak is observed at 515 K. In agreement with the diffraction studies, this is due to reaction 6 between KBH_4 and K_2ZnCl_4 causing release of B_2H_6 and H_2. The observed mass losses are 1.45 and 1.87 wt % for the samples **B2** and **B4**, respectively, which is in agreement with the higher amount of KBH_4 in the **B4** sample.

The total mass losses are 5.13 and 5.07 wt % for the samples **B2** and **B4**, respectively. For both samples, this constitutes more than the H_2 content calculated from the nominal sample composition (3.20 and 4.06 wt % H_2 for the samples **B2** and **B4**, respectively). This indicates that not only hydrogen but also boranes, most likely B_2H_6, are evolving in reactions 4 and 6. The total weight content of B_2H_6 + H_2 in the samples is 12.16 and 14.94 wt % for the samples **B2** and **B4**, respectively. Hence, the samples are not fully decomposed on heating to 773 K, most likely due to the high stability of the $K(BH_4)_{1-x}Cl_x$ solid solution. A sharp endothermic peak observed in both samples at 685 K is due to K_2ZnCl_4 decomposition.

CONCLUSIONS

Three novel alkali metal−transition metal borohydrides/chlorides are described in the KBH_4-ZnCl_2 system; i.e., $KZn(BH_4)_3$ and $K_2Zn(BH_4)_xCl_{4-x}$ form in ball-milled KBH_4:$ZnCl_2$ mixtures with molar ratios from 1.5:1 up to 3:1, while $K_3Zn(BH_4)_xCl_{5-x}$ forms only in the 2:1 mixture after longer milling times. The new compounds have been studied by a combination of in situ synchrotron powder diffraction, thermal analysis, Raman spectroscopy, and DFT calculations.

Rhombohedral $KZn(BH_4)_3$ contains an anionic complex $[Zn(BH_4)_3]^-$ with D_3 (32) symmetry, located inside a rhombohedron K_8. It is similar to a monoclinic $NaZn(BH_4)_3$ where the complex anion is located in a strongly deformed tetragonal prism. $KZn(BH_4)_3$ contains 8.1 wt % of hydrogen and decomposes at ∼385 K with a release of hydrogen and diborane. The decomposition temperature is much lower than for KBH_4, and it is similar to other Zn-based bimetallic borohydrides like $MZn_2(BH_4)_5$ (M = Li, Na) and $NaZn(BH_4)_3$.

Monoclinic $K_2Zn(BH_4)_xCl_{4-x}$ contains a tetrahedral $Zn(BH_4)_xCl_{4-x}$ unit which may be rationalized as a complex anion $[Zn(BH_4)_xCl_{4-x}]^{2-}$ based on the analysis of splitting of the B−H stretching mode. The complex anion is located inside an Edshammar polyhedron (pentacapped trigonal prism) K_{11}. The compound is a monoclinically distorted variant of the paraelectric orthorhombic *ht*-phase of K_2ZnCl_4 (structure type K_2SO_4). Similar compounds are observed also in related systems containing Mg, Mn, or Cd. During decomposition $K_2Zn(BH_4)_xCl_{4-x}$ releases BH_4 starting from 395 K, forming Zn and KBH_4. As the reaction proceeds and x decreases, the monoclinic distortion of $K_2Zn(BH_4)_xCl_{4-x}$ diminishes, and the structure transforms at 445 K into the orthorhombic *ht*-phase of K_2ZnCl_4.

Tetragonal $K_3Zn(BH_4)_xCl_{5-x}$ is a substitutional and deformation variant of the tetragonal ($I4/mcm$) Cs_3CoCl_5 structure type. Its structure is not fully characterized, and the most probable symmetry is that of s.g. $P4_2/ncm$. A similar compound with

the symmetry of another maximal subgroup of $I4/mcm$ was recently observed in a related system containing Mg. $K_3Zn(BH_4)_xCl_{5-x}$ decomposes nearly at the same temperature as $KZn(BH_4)_3$, i.e., at ~400 K, with a formation of $K_2Zn(BH_4)_xCl_{4-x}$ and KBH_4, indicating that the compound is an adduct of the two latter compounds.

■ ASSOCIATED CONTENT

Supporting Information. Tables of atomic positions; representative Rietveld refinement profiles; crystal data as CIF files. This material is available free of charge via the Internet at http://pubs.acs.org.

■ AUTHOR INFORMATION

Corresponding Author
*E-mail: radovan.cerny@unige.ch.

■ ACKNOWLEDGMENT

TRJ and DBR thank the Danish Research Council for Nature and Universe (Danscatt), the Danish National Research Foundation (Centre for Materials Crystallography), the Danish Strategic Research Council (Centre for Energy Materials), and the Carlsberg Foundation for funding. This work was supported by the Swiss National Science Foundation. L.S. wishes to express his thanks to Slovak Grant Agency VEGA for financial support under the contract no. 2/0150/09. The authors acknowledge SNBL for the beamtime allocation.

■ REFERENCES

(1) Nakamori,Y.; Orimo, S. In *Solid-State Hydrogen Storage, Materials and chemistry*; Walker, G., Ed.; Woodhead Publishing Ltd., 2008; pp 420−449.
(2) Ravnsbæk, D. B.; Filinchuk, Y.; Černý, R.; Jensen, T. R. *Z. Kristallogr.* **2010**, *225*, 557–569.
(3) Li, H.-W.; Orimo, S.; Nakamori, Y.; Miwa, K.; Ohba, N.; Towata, S.; Züttel, A. *J. Alloys Compd.* **2007**, *446−447*, 315–318.
(4) Hagemann, H.; Černý, R. *Dalton Trans.* **2010**, *39*, 6006–6012.
(5) Schlesinger, H. I.; Burg, A. B. *Chem. Rev.* **1942**, *31*, 1–41.
(6) Semenko, K. N.; Kravchenko, O. V.; Polyakova, V. B. *Russ. Chem. Rev.* **1973**, *42*, 1–13.
(7) Nöth, H. *Angew. Chem.* **1961**, *73*, 371–383.
(8) Marks, T. J.; Kolb, J. R. *Chem. Rev.* **1977**, *77*, 263–293.
(9) James, B. D.; Wallbridge, M. G. H. *Prog. Inorg. Chem.* **1970**, *11*, 99–231.
(10) Hagemann, H.; Longhini, M.; Kaminski, J. W.; Wesolowski, T. A.; Černý, R.; Penin, N.; Sorby, M. H.; Hauback, B. C.; Severa, G.; Jensen, C. M. *J. Phys. Chem. A* **2008**, *112*, 7551–7555.
(11) Černý, R.; Severa, G.; Ravnsbæk, D.; Filinchuk, Y.; D'Anna, V.; Hagemann, H.; Haase, D.; Jensen, C. M.; Jensen, T. R. *J. Phys. Chem. C* **2010**, *114*, 1357–1364.
(12) Černý, R.; Ravnsbæk, D.; Severa, G.; Filinchuk, Y.; D'Anna, V.; Hagemann, H.; Haase, D.; Skibsted, J.; Jensen, C. M.; Jensen, T. R. *J. Phys. Chem. C* **2010**, *114*, 19540–19549.
(13) Ravnsbæk, D.; Filinchuk, Y.; Cerenius, Y.; Jakobsen, H. J.; Besenbacher, F.; Skibsted, J.; Jensen, T. R. *Angew. Chem., Int. Ed.* **2009**, *48*, 6659–6663.
(14) Černý, R.; Ki Chul Kim; Penin, N.; D'Anna, V.; Hagemann, H.; Sholl, D. S. *J. Phys. Chem. C* **2010**, *114*, 19127–19133.
(15) Lindemann, I.; Domènech Ferrer, R.; Dunsch, L.; Filinchuk, Y.; Černý, R.; Hagemann, H.; D'Anna, V.; Lawson Daku, L. M.; Schultz, L.; Gutfleisch, O. *Chem.—Eur. J.* **2010**, *16*, 8707–8712.
(16) Lindemann, I.; Domènech Ferrer, R.; Dunsch, L.; Černý, R.; Hagemann, H.; D'Anna, V.; Filinchuk, Y.; Schultz, L.; Gutfleisch, O. *Faraday Discuss.* **2011**, *151*, 231–242.
(17) Ravnsbæk, D.; Sørensen, L. H.; Filinchuk, Y.; Reed, D; Book, D; Cerenius, Y.; Jakobsen, H. J.; Besenbacher, F.; Skibsted, J.; Jensen, T. R. *Eur. J. Inorg. Chem.* **2010**, 1608–1612.
(18) Ravnsbæk, D. B.; Ley, M. B.; Lee, Y.-S.; Hagemann, H.; D'Anna, V.; Cho, Y. W.; Filinchuk, Y.; Jensen, T. R. 2011, *submitted*.
(19) (a) Mosegaard, L.; Møller, B.; Jørgensen, J.-E.; Filinchuk, Y.; Cerenius, Y.; Hanson, J.; Dimasi, E.; Besenbacher, F.; Jensen, T. *J. Phys. Chem. C* **2008**, *112*, 1299–1303. (b) Arnbjerg, L. M.; Ravnsbæk, D. B.; Filinchuk, Y.; Vang, R. T.; Cerenius, Y.; Besenbacher, F.; Jørgensen, J.-E.; Jakobsen, H. J.; Jensen, T. R. *Chem. Mater.* **2009**, *21*, 5772–5782.
(20) Černý, R.; Penin, N.; D'Anna, V.; Hagemann, H.; Durand, E.; Ruzicka, J. *Acta Mater.* **2011**, *59*, 5171–5180.
(21) Lee, J. Y.; Ravnsbæk, D.; Lee, J. S.; Kim, Y.; Cerenius, Y.; Shim, J.-S.; Jensen, T. R.; Hur, N. W.; Cho, Y. W. *J. Phys. Chem. C* **2009**, *113*, 15080–15086.
(22) Hagemann, H.; D'Anna, V.; Rapin, J. P.; Černý, R.; Filinchuk, Ya.; Ki Chul Kim Sholl, D. S.; Parker, S. F. *J. Alloys Compd.* **2011**, *509*, S688–S690.
(23) Bardají, E. G.; Zhao-Karger, Z.; Boucharat, N.; Nale, A.; van Setten, M. J.; Lohstroh, W.; Röhm, E.; Catti, M.; Fichtner, M. *J. Phys. Chem. C* **2011**, *115*, 6095–6101.
(24) Hagenmuller, P.; Rault, M. *C. R. Acad. Sci.* **1959**, *248*, 2758–2760.
(25) Mikheeva, V. I.; Mal'tseva, N. N.; Alekseeva, L. S. *Russ. J. Inorg. Chem.* **1968**, *13*, 682–685.
(26) Schouwink, P.; D'Anna, V.; Ley, M. B.; Lawson Daku, L. M.; Jensen, T. R.; Hagemann, H.; Černý, R., submitted.
(27) Ravnsbæk, D. B.; Sørensen L. H.; Filinchuk, Y., Besenbacher, F.; Jensen, T. R. 2011, submitted.
(28) Hammersley, A. P.; Svensson, S. O.; Hanfland, M.; Fitch, A. N.; Häusermann, D. *High Pressure Res.* **1996**, *14*, 235–248.
(29) Quilinchini, M.; Bernede, P.; Lefebvre, J.; Schweiss, P. *J. Phys.: Condens. Matter* **1990**, *2*, 4543–4558.
(30) Favre-Nicolin, V.; Černý, R. *J. Appl. Crystallogr.* **2002**, *35*, 734–743.
(31) Menary, J. W. *Acta Crystallogr.* **1955**, *8*, 840.
(32) Coelho, A. A. TOPAS-Academic; http://members.optusnet.com.au/~alancoelho.
(33) Villars, P.; Cenzual, K. *Pearson's Crystal Data*, Release 2010/2011; ASM International, Materials Park, Ohio, USA, 2011.
(34) Spek, A. L. *PLATON*; University of Utrecht: The Netherlands, 2006.
(35) Efron, B.; Tibshirani, R. *Stat. Sci.* **1986**, *1*, 54–77.
(36) Kresse, G.; Hafner, J. *Phys. Rev. B* **1993**, *48*, 13115–13118.
(37) (a) Kresse, G.; Furthmüller *J. Phys. Rev. B* **1996**, *54*, 11169–11186. (b) Kresse, G.; Furthmüller *Comput. Mater. Sci.* **1996**, *6*, 15–50.
(38) Perdew, J. P.; Wang, Y. *Phys. Rev. B* **1992**, *45*, 13244–13249.
(39) Blöchl, P. E. *Phys. Rev. B* **1994**, *50*, 17953–17979.
(40) Kresse, G.; Joubert, J. *Phys. Rev. B* **1999**, *59*, 1758–1775.
(41) Kresse, G.; Hafner, J. *J. Phys.: Condens. Matter* **1994**, *6*, 8245–8527.
(42) Teter, M. P.; Payne, M. C.; Allan, D. C. *Phys. Rev. B* **1989**, *40*, 12255–12263.
(43) Bylander, D. M.; Kleinman, L.; Lee, S. *Phys. Rev. B* **1990**, *42*, 1394–1403.
(44) Hafner, J. *J. Mol. Struct.* **2003**, *651−653*, 3–17.
(45) Portmann, S.; Luthi, H. P. *Chimia* **2000**, *54*, 766–769.
(46) Powell, H. M.; Wells, A. F. *J. Chem. Soc.* **1935**, 359–362.
(47) Al-Kahtani, A.; Williams, D. L.; Nibler, J. W.; Sharpe, S. W. *J. Phys. Chem. A* **1998**, *102*, 537–544.
(48) (a) Filinchuk, Y.; Chernyshov, D.; Dmitriev, V. *Z. Kristallogr.* **2008**, *223*, 649–659. (b) Filinchuk, Y.; Chernyshov, D.; Dmitriev, V. In *Boron hydrides, high potential hydrogen storage materials*; Demirci, U.B.; Miele, P., Eds.; Nova Publishers, 2010a; arXiv: abs/1003.5378.
(49) Ravnsbæk, D.; Frommen, C.; Reed, D; Filinchuk, Y.; Sørby, M.; Hauback, H. J.; Jakobsen, D.; Book, D; Besenbacher, F.; Skibsted, J.; Jensen, T. R. *J. Alloys Compd.* **2011**, *509S*, 5698–5704.

(50) Abrikosov, N. K.; Wasserman, A. M.; Poretskaya, L. V. *Dokl. Akad. Nauk SSSR* **1958**, *123*, 279−281 (in Russian).
(51) Edshammar, L. E., Dissertation, University of Stockholm, 1969.
(52) (a) Makarov, E. S. *Izv. Akad. Nauk SSSR (Ser. Khim.)* **1944**, 29. (b) Laves, F.; Wallbaum, H. J. *Z. Angew. Mineral.* **1942**, *4*, 17–46.
(53) Stöwe, K. *Z. Kristallogr.* **2004**, *219*, 359–369.
(54) Kovaleva, I. S.; Kuznetsova, I. Y.; Fedorov, V. A.; Boguslavskii, A. A.; Lotfullin, R. S. *Russ. J. Inorg. Chem.* **1990**, *35*, 100–103.
(55) Avery, J. S.; Burbridge, C. D.; Goodgame, D. M. L. *Spectrochim. Acta A* **1968**, *24*, 1721–1726.
(56) Jeon, E.; Cho, Y. W. *J. Alloys Compd.* **2006**, *422*, 273–275.
(57) Brandenburg, K. *DIAMOND*, version 3.2.g; Crystal Impact GbR: Bonn, Germany, 2011.